

Evaluation of Fatigue Crack Front Shape for a Specimen with Finite Thickness

Zhuang He^{1, a}, Andrei Kotousov¹ and Ricardo Branco²

¹*School of Mechanical Engineering, the University of Adelaide, SA 5005 Australia*

²*Department of Mechanical Engineering, Polytechnic Institute of Coimbra, Portugal*

Abstract. Two-dimensional elastic or elasto-plastic models dominate the current fatigue crack growth assessment and life prediction procedures for plate components with through-the-thickness cracks. However, as demonstrated in many theoretical and experimental papers, the stress field near the crack tip is always three-dimensional and the fatigue crack front is not straight. In this paper, we develop a simplified approach for the evaluation of the front shapes of through-the-thickness fatigue cracks. We validate this approach against experimental results available from published papers.

1 Introduction

Propagation of through-the-thickness cracks in plates is often treated as a two-dimensional process. In other words, the crack front is assumed to be straight and the variation of the stresses along the thickness direction to be negligible. These common assumptions essentially reduce the dimensionality of the problem, significantly simplify the modelling approaches, and in many cases provide a satisfactory solution useful for analysis of practical problems [1]. Despite a large number of three-dimensional analytical, numerical and experimental studies carried out over the past decade [2], it is still unclear how adequate these common assumptions and simplifications are, and what influence the account for the crack front shapes has on fatigue life predictions. Therefore, this paper is concerned with the three-dimensional analysis of fatigue crack front shapes. Recent numerical studies closely related to the current work will be briefly presented next.

Branco and Antunes [3] developed a comprehensive iterative numerical procedure to study the shape evolution of fatigue cracks in plates based on the 3D finite element method. This automatic iterative procedure was modified and advanced in a number of subsequent papers [4-6]. The crack shape evolution in this procedure is governed by the effective stress intensity factor, which takes into account the plastically-induced crack closure phenomenon. The predictions of fatigue crack front shapes from these numerical simulations were compared and showed good agreement with outcomes of the corresponding fatigue tests. However, this numerical procedure relies on a number of parameters, which are not directly related to the physical problem but rather to the computational procedure itself [7]. In addition, there is not a simple and transparent way to independently reproduce or verify the

computational procedure as well as reported numerical results and conclusions. Therefore, in this paper we suggest a simplified method to the calculation of stable fatigue crack front shapes, which avoids many of the existing uncertainties and difficulties, experienced by the current numerical procedures.

The suggested method is based on a previously developed analytical approach for the analysis of plasticity-induced closure for cracks in plates of finite thickness [8]. The analytical approach provides the values of the stress intensity factor along the crack front at the mid-point and for points close to the free surface. The crack front shapes are approximated by a continuous set of parametric curves similar to the numerous previous studies for circumferential or elliptical cracks. By using the linear-elastic finite element method we analyse the parametric curves and identify the closest shape, which satisfies the stable (or steady state) condition of fatigue crack propagation. The stable conditions require the effective stress intensity factor to be a constant value along the plate thickness [9]. It is believed that the developed method is capable to capture the general tendencies of the crack front shape evaluation.

2 Outline of the Method

In this section we briefly discuss the analytical approach for the evaluation of the effective stress intensity factor for through-the-thickness cracks in finite thickness plates and outline the main features of the parametric finite element modelling.

2.1 Analytical Approach

^a Corresponding author: zhuang.he@adelaide.edu.au

It is well known that the crack growth rate for a given material can vary significantly with the applied load ratio and the thickness of the plate or shell component. In the early 1970s, Elber [10] suggested that premature closure of the crack surfaces, whilst the applied load is still tensile, will alter the crack driving force and thus the crack growth rate. Referred to as crack closure, these arguments are frequently utilized to analyse and explain the influence of the load ratio [11] and specimen thickness [12] on the fatigue crack growth rate.

The normalized load ratio parameter U (or the normalized effective stress intensity factors) is often used to describe the effects of loading and plate geometry on crack closure. This parameter is defined as [13]:

$$U = \Delta K_{\text{eff}} / \Delta K. \quad (1)$$

Here, ΔK_{eff} is the effective stress intensity factor range and $\Delta K = (K_{\text{max}} - K_{\text{min}})$ is the applied stress intensity factor range. The stress intensity factors K_{max} and K_{min} are the maximum and minimum values, respectively, experienced for a given load cycle and the load ratio is therefore given by $R = K_{\text{min}} / K_{\text{max}}$. The crack growth rate is then a function of the effective stress intensity factor range:

$$\Delta K_{\text{eff}} = K_{\text{max}} - K_{\text{op}} = U \Delta K. \quad (2)$$

Here, K_{op} is the opening load stress intensity factor, which corresponds to the minimum load at which the crack faces will be fully separated. Many models have been developed in the past [14, 15]. Below we present an analytical model [16], which directly incorporates the plate thickness and will be used in conjunction with parametric finite element calculations as outlined above. In accordance with this model, the parameter U for mode I loading under small-scale yielding conditions can be approximated from the following equations:

$$U(R, \eta) = A(\eta) + B(\eta)R + C(\eta)R^2. \quad (3)$$

with functions A , B and C are given as the following equations:

$$A(\eta) = 0.446 + 0.266 \times e^{-0.41\eta}. \quad (4a)$$

$$B(\eta) = 0.373 + 0.354 \times e^{-0.235\eta}. \quad (4b)$$

$$C(\eta) = 0.2 - 0.667 \times e^{-0.515\eta}. \quad (4c)$$

where the dimensionless parameter

$$\eta = K_{\text{max}} / (\sigma_f \times h^{0.5}). \quad (5)$$

In Eq. 5, h is half plate thickness and the flow stress σ_f is taken as the average of yield strength and ultimate tensile strength of the material.

The above equations have been obtained within the first order plate theory, fundamental solution for edge dislocation and utilizing Budiansky-Hutchinson crack closure model [17]. The results which correspond to the

classical two-dimensional theories (or plane stress or plane strain conditions) can be obtained as a limiting cases of very thin or very thick plates, i.e. when $\eta \rightarrow \infty$ or $\eta \rightarrow 0$, respectively. The details of the derivation of these equations can be found in the original paper by Codrington and Kotousov [16].

2.2 Parametric Equation for Crack Front Shape

Similar to other numerous approaches, which have been previously implemented to simulate fatigue crack growth and shape evaluation of circumferential and elliptic cracks [18, 19] and for simplicity reasons, the shape of the front crack is approximated by the following equations:

$$x = \begin{cases} 0, z < \beta \\ \alpha(z - \beta)^2, z \geq \beta \end{cases}. \quad (6)$$

Here, the coordinate system is set at the middle of the plate and x is the direction of the crack propagation and z – axis is along the transverse (or thickness) direction. From an analysis of fatigue crack shapes for relatively plastic materials the parameter is set at $\beta \approx 0.2h$ [20]. Thus, α is the only parameter in Eq. 6, which needs to be determined from the finite element calculations to specify the particular shape of the crack front.

2.3 Numerical Procedure

The numerical procedure comprises three main steps:

Step 1: In the beginning, a guess value of parameter α in Eq. 6 is selected and a corresponding finite element model with the crack front shape given by Eq. 6 is developed. From linear elastic three-dimensional finite element analysis the distribution of the maximum stress intensity factors along the thickness direction under the maximum loading conditions are obtained in accordance with the techniques developed in Harding et al. [21] and Kotousov et al. [22].

Step 2: Further, using the analytical approach as described above, see Eqs 2 – 5, the effective stress intensity factors in the middle and at a location in a close vicinity to the free surface are calculated. This location is selected to avoid the effect of 3D corner singularities ($\sim 0.1h$ from the free surface) [23-25]. For this location the stress state is assumed to be dominated by plane stress conditions, which corresponds to $h = 0$ or $\eta \rightarrow \infty$ in Eqs 3 – 5.

Step 3: Finally, these two effective stress intensity factors are compared and a new guess value of α is intelligently selected to reduce the difference between these values of the effective stress intensity factors. The uniform effective stress intensity factor across the thickness corresponds to a stable fatigue crack front as all segments of the crack front grow with the same rate. The iteration is repeated until the difference between the two calculated values drops normally below 5%, usually, five – six iterations are sufficient to achieve such accuracy.

All numerical calculations are conducted with ANSYS 14.5. Symmetry boundary conditions on the problem symmetry planes are enforced to reduce the size of the finite element model. Thirty key points are specified to define the crack front and the standard spline interpolation is applied between these points. The model is meshed with 20 node hexahedral elements. A higher mesh density is applied in vicinity of the crack front (as shown in Fig. 1), while the area far away from the crack front is coarsened to reduce the computational time.

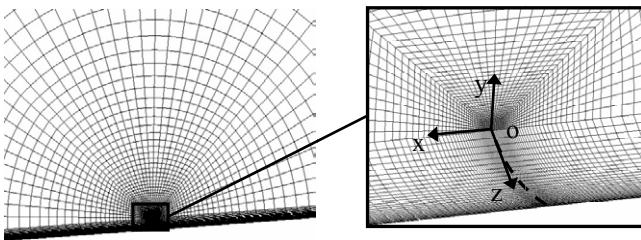


Figure 1. Mesh in vicinity of the crack front.

3 Comparison with Experimental Data

In order to check the effectiveness and accuracy of the developed method, the calculated stable crack front shapes were compared with selected experimental results [26] for middle cracked tension specimens of two distinct thicknesses of 2.29 mm and 6.35 mm. A detailed description of the specimen geometries, material properties and details of the cyclic loading conditions are listed in Table 1. The outcomes of the calculations of the crack front shapes are presented in Fig. 2, together with the experimental measurements. As can be seen from this figure, the modelling predictions are in good agreement with the experimental results. It shows that plate thickness is a main factor affecting the shape of the fatigue crack front, with an increase of the plate thickness and at the same all other conditions the crack front curvature is decreased (noting that the horizontal axis in Fig. 2 represents the normalized distance along the thickness direction z).

Table 1: Geometries, material properties and cyclic loading conditions for Centre Cracked Tension specimens.

Specimen geometries [mm]			Material properties (2024-T3 Al)		Cyclic loading conditions	
Thickness (2h)	2.29	6.35	Young's modulus (E)	73 [GPa]	Frequency	10 [Hz]
Length (2L)	200		Poisson's ratio (ν)	0.33	Load ratio (R)	0.05
Width (2W)	100		Flow stress (σ _f)	400 [MPa]	Applied stress (σ _z)	118 [MPa]
Crack length (2a)	28					

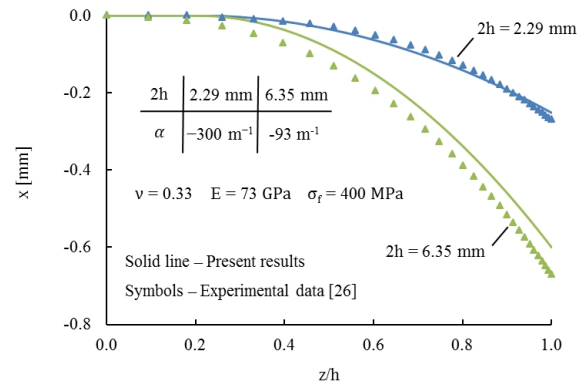


Figure 2. Comparison between calculated and experimental crack front shapes.

4 Conclusion

Many difficulties in the selection of computational parameters in the direct FE based numerical calculation of the fatigue crack fronts are the main motivation behind the current work, which was seeking a balance between the computational effort and the accuracy of the calculations. A simplified method has been developed and partially validated against the previously published results. This method is based on a number of implicit and explicit assumptions and utilizes the earlier developed model for plastically-induced crack closure as well as a linear-elastic 3D FE modelling. The application of the analytical model for calculation of the effective stress intensity factor, based on the classical plasticity-induced crack closure, allows for a significant reduction in the complexity of the computational procedure.

References

1. A. Kotousov: Int. J. Solids Struct. Vol. 44 (2007), p. 8259-8273.
2. L.P. Pook: Eng. Fract. Mech. Vol. 77 (2013), p. 1619-1630.
3. R. Branco, F.V. Antunes: Eng. Fract. Mech. Vol. 75 (2008), p. 3020-3037.
4. F.V. Antunes, R. Branco, J.D. Costa and D.M. Rodrigues: Fatigue Fract. Eng. Mater. Struct. Vol. 33 (2010), p. 673-686.
5. R. Branco, F.V. Antunes, L.H. Ricardo and J.D. Costa: Finite Elem. Anal. Des. Vol. 50 (2012), p. 147-160.
6. R. Branco, F.V. Antunes and J.D. Costa: Key Eng. Mater. Vol. 560 (2013), p. 107-127.
7. X.B. Lin, R.A. Smith: Eng. Fract. Mech. Vol. 63 (1999), p. 503-522.
8. A. Kotousov, J. Codrington: *Structural Failure Analysis and Prediction Methods for Aerospace Vehicles and Structures* (Bentham Science Publishers, 2010).
9. C.Y. Hou: Int. J. Fatigue Vol. 33 (2011), p. 719-726.
10. W. Elber: Eng. Fract. Mech. Vol. 2 (1970), p. 37-45.
11. R. Kumar, K. Singh: Eng. Fract. Mech. Vol. 50 (1995), p. 377-384.

12. J.D.M. Costa, J.A.M. Ferreira: *Theor. Appl. Fract. Mech.* Vol. 30 (1998), p. 65-73.
13. R. Jones: *Fatigue Fract. Eng. Mater. Struct.* Vol. 37 (2014), p. 463-483.
14. T. Machniewicz: *Fatigue Fract. Eng. Mater. Struct.* Vol. 36 (2013), p. 361-373.
15. K.F. Walker, J.C. Newman: *Fatigue Fract. Eng. Mater. Struct.* Vol. 37 (2014), p. 659-670.
16. J. Codrington, A. Kotousov: *Mech. Mater.* Vol. 41 (2009), p. 165-173.
17. B. Budiansky, J.W. Hutchinson: *J. Appl. Mech.* Vol. 45 (1978), p. 267-276.
18. M.A. Mahmoud, A. Hosseini: *Eng. Fract. Mech.* Vol. 24 (1986), p. 897-913.
19. R.A. Smith, J.F. Cooper: *Int. J. Press. Vessels Pip.* Vol. 36 (1989), p. 315-326.
20. S. Seitzl, P. Hutar, T.E. Garcia and A. Fernandez-Canteli: *Applied and Computational Mechanics* Vol. 7 (2013), p. 53-64.
21. S. Harding, A. Kotousov, P. Lazzarin and F. Berto: *Int. J. Fract.* Vol. 164 (2010), p. 1-14.
22. A. Kotousov, P. Lazzarin, F. Berto and P.L. Pook: *Eng. Fract. Mech.* Vol. 108 (2013), p. 65-74.
23. A. Kotousov: *Int. J. Solids Struct.* Vol. 47 (2010), p. 1916-1923.
24. A. Kotousov, P. Lazzarin, F. Berto and S. Harding: *Eng. Fract. Mech.* Vol. 77 (2010), p. 1665-1681.
25. Z. He, A. Kotousov and F. Berto: *Fatigue Fract. Eng. Mater. Struct.* (2015) Published online.
26. H. Hosseini-Toudeshky, G. Sadeghi and H.R. Daghyani: *Compos. Struct.* Vol. 71 (2005), p. 401-406.